

S-Wave Single Heavy Baryons with Spin-3/2 at Finite Temperature

K. Azizi^{1,2}, A. Türkan³

¹*Department of Physics, University of Tehran, North Karegar Avenue, Tehran 14395-547, Iran*

²*Department of Physics, Doğuş University, Acıbadem-Kadıköy, 34722 Istanbul, Turkey*

³*Özyeğin University, Department of Natural and Mathematical Sciences, Çekmeköy, 34794 Istanbul, Turkey*

(ΩDated: April 17, 2020)

The thermal behavior of the spectroscopic parameters of the S-wave single heavy baryons Σ_c^* , Ξ_c^* and Ω_c^* with spin-3/2 are investigated in QCD at finite temperature. We analyze the variations of the mass and residue of these baryons taking into consideration the contributions of QCD thermal condensates up to dimension eight in Wilson expansion. At finite temperature, due to the breakdown of the Lorentz invariance by the choice of reference frame and presence of an extra $O(3)$ symmetry, some new four-dimensional operators come out in the form of the fermionic and gluonic parts of the energy momentum tensor that are taken into account in the calculations. Our analyses show that at lower temperatures, the parameters of baryons under consideration are not affected by the medium. These parameters, however, show rapid variations with respect to temperature at higher temperatures near to a pseudo-critical temperature, after which the baryons are melted. The results of the masses and residues at $T \rightarrow 0$ limit are compatible with the available experimental data and predictions of other theoretical studies.

I. INTRODUCTION

With the rising number of experimental data on charmed and bottom baryons, the interest in the investigation of heavy baryons has increased, considerably. Before giving the details of the experimental studies on heavy baryons, it would be useful to give some theoretical information. The Quark Model is one of the most successful tools to classify the mesons and baryons. The traditional single heavy baryons (Qqq) consist of one heavy ($Q = b$ or c) and two light quarks ($q = u, d$ or s). The mass of heavy quark is very large compared to the light quark masses and the light degrees of freedom form a diquark qq , which orbits the nearly static heavy Q quark. Therefore, infinitely heavy mass limit ($m_Q \rightarrow \infty$) for the heavy quark is utilized to classify the single heavy baryons [1, 2]. In this case, for the two light quarks, the total flavor-spin wave function has to be symmetric because their color wave function is antisymmetric. Hence there are two different representations for the S-wave heavy baryons ($\mathbf{3} \otimes \mathbf{3} = \bar{\mathbf{3}} \oplus \mathbf{6}$): antisymmetric $\bar{\mathbf{3}}$ or symmetric $\mathbf{6}$. The antitriplet ($\bar{\mathbf{3}}$) of baryons contain only spin-1/2 states while the sextet ($\mathbf{6}$) of baryons contain both spin-1/2 and spin-3/2 states. In this study, we investigate the thermal properties of the single heavy bottom/charmed spin-3/2 sextet states: The members for charmed baryons are shown in Figure 1.

Experimentally, the $\frac{1}{2}^+$ antitriplet (Λ_c^+ , Ξ_c^+ , Ξ_c^0) states, the $\frac{1}{2}^+$ sextet (Ω_c , Σ_c , Ξ_c') baryons and the $\frac{3}{2}^+$ sex-

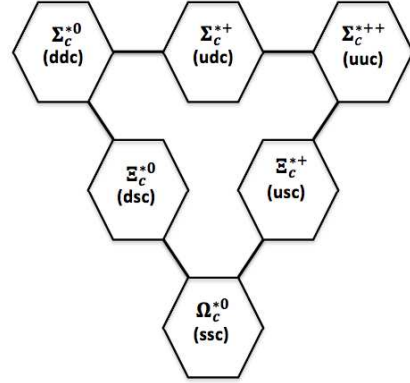


FIG. 1: The sextet representation of single charmed baryons with total spin-3/2. The same picture is valid for bottom baryons with the replacement $c \rightarrow b$.

tet (Ω_c^* , Σ_c^* , Ξ_c^*) resonances have been observed in the charmed sector while the only Λ_b , $\Sigma_b^{(*)}$, $\Xi_b^{(*)}$ and Ω_b have been discovered in the bottom picture [3]. Some history of discoveries are in order: In 2006 the CDF collaboration reported observation of Λ_b [4] and Ω_c^* discovered by the Babar collaboration [5]. The CDF collaboration reported the first observation of Σ_b and Σ_b^* baryons later [6]. The D0 collaboration declared the observation of Ξ_b [7] and it was confirmed by CDF in a short time [8]. The observation of ground and excited states of Ξ_c were proclaimed by Belle and BABAR collaborations [9, 10]. Ξ_c^* observed by Belle in 2008 [11] and discovery of Ξ_b^* was reported by

CMS and LHCb collaborations [12, 13].

On the other hand, various theoretical studies in vacuum have been utilized to investigate the spectroscopic parameters of single heavy baryons. In 1982 Shuryak primarily calculated the heavy baryon masses via QCD sum rule [14]. In Ref. [15] Capstick and Isgur examined the heavy baryon systems in a quark potential model. Bagan et al. investigated the heavy baryons by taking into account the separation of negative and positive parity contributions [16]. Grozin and Yakovlev evaluated the masses of Λ_Q and $\Sigma_Q^{(*)}$ using the heavy quark effective theory (HQET) [17]. Charmed baryons were investigated in Chiral perturbation theory by Savage and also results were extended for b-baryons in the same study [18]. Roncaglia et al. in Ref [19] estimated the heavy baryon masses with one/two heavy quark/quarks in the framework of Feynman-Hellman theorem. In Ref. [20] Jenkins studied the masses of heavy baryons in the $1/m_Q$ and $1/N_c$ expansions. The $1/m$ corrections to heavy baryon masses were calculated by Dai et al. in the framework of the HQET [21]. QCD sum rule for heavy baryons at leading order in $1/m_Q$ and at next to the leading order in α_s were evaluated by Groote et al. in Ref. [22]. Wang et al. improved the analysis for the Λ_Q and Σ_Q baryon masses to order Λ_{QCD}/m_Q from QCD sum rule [23]. Mathur et al. predicted the mass spectrum of charmed and bottom baryons from Lattice QCD [24]. Wang and Huang in Ref. [25] studied the mass, coupling constant, and Isgur-Wise function for ground-state heavy baryons within the framework of HQET by taking into account both the two and three-point correlation functions. Ebert et al. computed heavy baryon masses in the heavy-quark light-diquark approximation in the framework of constituent quark model [26]. Garcilazo et al. solved exactly the three quark problem via Faddeev method in momentum space [27]. In Ref. [28] Zang and Huang calculated the charm and bottom baryon masses up to operator dimension six in operator product expansion (OPE) by the help of the QCD sum rule approach. The mass and residue of Ω_c^* and Ω_b^* with spin parity $3/2^+$ were studied by Wang via QCD sum rule [29]. A quark model was applied to the spectrum of baryons containing one heavy baryon by Roberts and Pervin [30]. Bottom baryon spectra were investigated using Faddeev method in momentum space by Valcarce et al. [31]. Liu et al. performed a systematic study of the masses of bottom baryons up to $1/m_Q$ in HQET [32]. Groote et al. computed the NLO perturbative corrections for the static

properties of heavy baryons [33]. In Ref. [34] the mass of Λ_Q and $\Sigma_Q^{(*)}$ baryons were calculated by Zhang and Huang via QCD sum rule taking into account operators up to dimension six. Using the coupled channel formalism, Gerasyuta and Matskevich calculated the S-wave bottom baryons masses [35]. In Ref. [36] Karliner et al. investigated the b-baryons in the quark model. In two-point and light cone QCD sum rule methods Aliev et al. studied the mass and magnetic moments of single heavy baryons with spin-3/2 [37]. Lewis and Shyn predicted the bottom baryon masses based on a $2 + 1$ flavor dynamical lattice QCD simulation [38]. The spin-3/2⁺ heavy and doubly heavy baryon states [39] were investigated by subtracting the contributions from the corresponding negative parity by Z. G. Wang. The mass spectra of heavy baryons were studied by the help of the motivated relativistic quark model by Ebert [40]. Kim et al. investigated the single heavy baryon mass based on the self-consistent Chiral quark soliton model in Ref. [41]. Finally, Azizi and Er studied the in-medium properties of spin-3/2 heavy baryons in nuclear matter using QCD sum rule in a dense medium [42].

Theoretical investigations of spectroscopic parameters of the single heavy baryons at finite temperature will help us better understand and analyze the results of heavy-ion collision experiments and gain valuable information on the internal structures of these baryons, behavior of these baryons near to a pseudo-critical temperature, possible phase transition/ crossover [43, 44] to/with quark gluon plasma (QGP) (adopted as a new phase of matter) as well as the perturbative and nonperturbative dynamics of QCD. At extreme temperatures, two different possibilities can be considered: crossover and phase transition. Many Lattice calculations predict that crossover occurs at $T_{pc} \approx 155 MeV$ [45, 46]. For the QGP phase transition, we need greater temperature values and there is no unique temperature to the phase transition of QGP. At short distances, to describe the strong interaction QCD is a suitable theory. However, the calculations of hadronic parameters including nonperturbative effects (occur in low energy scale) usually need some nonperturbative phenomenological models. Many phenomenological models are available in the literature: QCD sum rule is one of the powerful ones among them. This method firstly suggested by Shifman, Vainshtein and Zakharov to investigate the vacuum properties of mesons [47] and then Ioffe [48] applied this method for baryons. The thermal version of the QCD sum rule was extended by Bochkarev

and Shaposhnikov [49]. In addition to the vacuum expectation values of quark and gluon condensates, their thermal forms and some new operators appear in the thermal version.

In this study, we investigate the temperature effects on the spectroscopic parameters of the ground state sextet baryons including single heavy quark and with spin-3/2 via thermal QCD sum rule method. Taking into account the additional operators coming from OPE due to breaking of the Lorentz invariance by the choice of the thermal rest frame, condensates up to dimension eight are considered. The article is arranged in the following form. In Sec. II, the in-medium sum rules for the mass and residues of the Σ_Q^* , Ξ_Q^* and Λ_Q^* single heavy baryons are obtained. In Sec. III the numerical analysis for the spectroscopic parameters under consideration is performed. The last section includes the summary and our concluding remarks.

II. CALCULATIONS

In this section, QCD sum rules for the spectroscopic parameters of the spin-3/2 Σ_Q^* , Ξ_Q^* and Ω_Q^* baryons are obtained at finite temperature. To this end, we start with the following two-point thermal correlation function:

$$\Pi_{\mu\nu}(q, T) = i \int d^4x e^{iq \cdot x} \langle \Psi | \mathcal{T} \{ J_\mu(x) \bar{J}_\nu(0) \} | \Psi \rangle, \quad (1)$$

where q is the four-momentum of the chosen baryon, Ψ is the ground state of the hot medium, \mathcal{T} denotes the time-ordering operator and $J_\mu(x)$ is the interpolating current of the single heavy baryon, B_{SH} .

As the standard procedures of the QCD sum rule, the correlation function given above can be calculated at different contexts. At large distances, it is evaluated in terms of the hadronic parameters such as the mass and residue of hadron. We call it the physical or hadronic representation of the correlator. The same correlator can be expressed in terms of the quark, gluon and mixed condensates by the help of the OPE at $q^2 \ll 0$ region. The computations in this way contain short distance effects. This representation, is generally called the OPE or QCD side of the correlation function. Finally, we match the two windows and compare the coefficients of the same Lorentz structures from both sides. To remove the unwanted contributions coming from the higher states and continuum, Borel transformation as well as continuum subtraction, supplied by the quark-hadron duality assumption at finite temperature, are performed. These

procedures bring some auxiliary parameters, which we fix them before making any numerical estimations on the physical quantities.

To obtain the physical side of the correlator, a complete set of intermediate state with the same quantum numbers and quark content as the chosen current is inserted between the interpolating currents in correlation function. This is followed by the integral over four- x , which leads to

$$\begin{aligned} & \Pi_{\mu\nu}^{Phys}(q, T) \\ &= - \frac{\langle \Psi | J_\mu(0) | B_{SH}(q, s) \rangle \langle B_{SH}(q, s) | J_\nu^\dagger(0) | \Psi \rangle}{q^2 - m_{B_{SH}}^2(T)} \\ &+ \text{contribution of higher states and continuum,} \end{aligned} \quad (2)$$

where $m_{B_{SH}}(T)$ is the temperature-dependent mass of the ground state of B_{SH} . The matrix element $\langle \Psi | J_\mu(0) | B_{SH}(q, s) \rangle$ is defined in terms of the temperature dependent residue, $\lambda_{B_{SH}}(T)$, as

$$\langle \Psi | J_\mu(0) | B_{SH}(q, s) \rangle = \lambda_{B_{SH}}(T) u_\mu(q, s), \quad (3)$$

where $u_\mu(q, s)$ is the Rarita-Schwinger spinor. The final form of the physical side can be obtained by inserting Eq. (3) into Eq. (2) and summing over the spins of the B_{SH} . The summation over Rarita-Schwinger spinors is performed using

$$\begin{aligned} & \sum_s u_\mu(q, s) \bar{u}_\nu(q, s) \\ &= - \left(\not{q} + m_{B_{SH}} \right) \left[g_{\mu\nu} - \frac{1}{3} \gamma_\mu \gamma_\nu \right. \\ & \left. - \frac{2 q_\mu q_\nu}{3 m_{B_{SH}}^2} + \frac{q_\mu \gamma_\nu - q_\nu \gamma_\mu}{3 m_{B_{SH}}} \right]. \end{aligned} \quad (4)$$

By using the above behest, we recast the physical side as

$$\begin{aligned} \Pi_{\mu\nu}^{Phys}(q, T) &= \frac{\lambda_{B_{SH}}^2(T) (\not{q} + m_{B_{SH}})}{q^2 - m_{B_{SH}}^2(T)} \left[g_{\mu\nu} - \frac{1}{3} \gamma_\mu \gamma_\nu \right. \\ & \left. - \frac{2 q_\mu q_\nu}{3 m_{B_{SH}}^2} + \frac{q_\mu \gamma_\nu - q_\nu \gamma_\mu}{3 m_{B_{SH}}} \right] + \dots, \end{aligned} \quad (5)$$

where $\lambda_{B_{SH}}^2(T) = \lambda_{B_{SH}}(T) \bar{\lambda}_{B_{SH}}(T)$. It should also be specified that the interpolating current $J_\mu(x)$ couples to both the spin-1/2 and spin-3/2 states. In this study, we only consider the contribution of spin-3/2 heavy baryons and we need to comb out the pollution of spin-1/2 state. These unwanted contributions can be eliminated in two different ways: 1) For spin-3/2 state, it should be introduced a projection operator which destroys the spin-1/2

contributions, 2) By a specific ordering of the Dirac matrices and remove the terms corresponding to the spin-1/2 particles (for more details see for instance [50]). The contribution of the spin-1/2 states can be traced using

$$\langle \Psi | J_\mu(0) | \frac{1}{2}(q) \rangle = [\kappa_1 q_\mu + \kappa_2 \gamma_\mu] u(q), \quad (6)$$

where κ_1 and κ_2 are some constants. By applying the condition $J_\mu \gamma^\mu = 0$ (for more details see [51]), we get κ_1 in terms of κ_2 . Hence,

$$\langle \Psi | J_\mu(0) | \frac{1}{2}(q) \rangle = \kappa_2 \left(\gamma_\mu - \frac{4}{m_{\frac{1}{2}}} q_\mu \right) u(q). \quad (7)$$

As is seen from Eq. (7), the pollution coming from spin-1/2 resonances are commensurate to either q_μ or γ_μ . To remove these contributions, the Dirac matrices are ordered as $\gamma_\mu \not{q} \gamma_\nu$ and terms proportional to q_μ or q_ν , also those beginning with γ_μ or ending with γ_ν are set to zero. Finally, the clean physical side of the correlator, in the Borel scheme, is obtained as

$$\begin{aligned} \hat{B}\Pi_{\mu\nu}^{Phys}(q, T) &= \lambda_{B_{SH}}^2(T) e^{-m_{B_{SH}}^2(T)/M^2} \not{q} g_{\mu\nu} \\ &+ \lambda_{B_{SH}}^2(T) m_{B_{SH}} e^{-m_{B_{SH}}^2(T)/M^2} g_{\mu\nu} \\ &+ \dots, \end{aligned} \quad (8)$$

where M^2 is the Borel parameter and dots denote the contributions of other structures as well as the higher states and continuum.

The next step is to calculate the OPE side of the correlation function. In deep Euclidean region, the correlation function is evaluated in terms of the quark and gluon degrees of freedom by the help of Wilson expansion. To achieve this goal, the basic point it to choose a suitable

interpolating current defining the particles under study. The interpolating current for spin-3/2 B_{SH} in a compact form can be written as [52–54]

$$\begin{aligned} J_\mu(x) &= A \epsilon_{abc} \left[\left(q_1^{aT}(x) C \gamma_\mu q_2^b(x) \right) Q^c(x) \right. \\ &+ \left(q_2^{aT}(x) C \gamma_\mu Q^b(x) \right) q_1^c(x) \\ &\left. + \left(Q^{aT}(x) C \gamma_\mu q_1^b(x) \right) q_2^c(x) \right], \end{aligned} \quad (9)$$

where A is the normalization constant, ϵ_{abc} is the anti-symmetric Levi-Civita tensor, a, b, c are color indices, $q_{1(2)}$ denotes the light quark (u, d or s), Q is the bottom (b) or charm (c) quark and C is the charge conjugation operator. The normalization constant A and the $q_{1(2)}$ quark for the considered baryons are given in Table I.

	$\Sigma_{b(c)}^{*+(++)}$	$\Sigma_{b(c)}^{*0(+)}$	$\Sigma_{b(c)}^{*- (0)}$	$\Xi_{b(c)}^{*0(+)}$	$\Xi_{b(c)}^{*- (0)}$	$\Omega_{b(c)}^{*- (0)}$
A	$\sqrt{1/3}$	$\sqrt{2/3}$	$\sqrt{1/3}$	$\sqrt{2/3}$	$\sqrt{2/3}$	$\sqrt{1/3}$
q_1	u	u	d	u	d	s
q_2	u	d	d	s	s	s

TABLE I: The light quark flavors for the single heavy baryons with spin-3/2 and the value of normalization constant A .

By inserting the explicit form of the interpolating current into the correlator and contracting all heavy and light quark fields via Wick's theorem, we get the correlation function in the case of $q_1 \neq q_2$ in terms of the thermal light(heavy) quark propagators, $S_{q(Q)}$, as

$$\begin{aligned} \Pi_{\mu\nu}^{OPE}(q, T) &= -\frac{2i}{3} \epsilon_{abc} \epsilon_{a'b'c'} \int d^4x e^{iq \cdot x} \left\{ S_Q^{cc'} Tr[S_{q_2}^{ba'} \gamma_\nu \tilde{S}_{q_1}^{ab'} \gamma_\mu] + S_{q_1}^{cc'} Tr[S_Q^{ba'} \gamma_\nu \tilde{S}_{q_2}^{ab'} \gamma_\mu] \right. \\ &+ S_{q_2}^{cc'} Tr[S_{q_1}^{ba'} \gamma_\nu \tilde{S}_Q^{ab'} \gamma_\mu] + S_Q^{ca'} \gamma_\nu \tilde{S}_{q_2}^{bb'} \gamma_\mu S_{q_1}^{ac'} + S_Q^{cb'} \gamma_\nu \tilde{S}_{q_1}^{aa'} \gamma_\mu S_{q_2}^{bc'} \\ &\left. + S_{q_1}^{cb'} \gamma_\nu \tilde{S}_{q_2}^{aa'} \gamma_\mu S_Q^{bc'} + S_{q_1}^{ca'} \gamma_\nu \tilde{S}_Q^{bb'} \gamma_\mu S_{q_2}^{ac'} + S_{q_2}^{ca'} \gamma_\nu \tilde{S}_{q_1}^{bb'} \gamma_\mu S_Q^{ac'} + S_{q_2}^{cb'} \gamma_\nu \tilde{S}_Q^{aa'} \gamma_\mu S_{q_1}^{bc'} \right\}. \end{aligned} \quad (10)$$

Some extra contractions arise because of the identical particles in the case of $q_1 = q_2 = q$, and the correlator is obtained as

$$\begin{aligned} \Pi_{\mu\nu}^{OPE}(q, T) &= \frac{i}{3} \epsilon_{abc} \epsilon_{a'b'c'} \int d^4x e^{iq \cdot x} \left\{ 2S_Q^{cc'} Tr[S_q^{bb'} \gamma_\nu \tilde{S}_q^{aa'} \gamma_\mu] + 2S_Q^{cc'} Tr[S_Q^{bb'} \gamma_\nu \tilde{S}_q^{aa'} \gamma_\mu] \right. \\ &+ 2S_q^{cc'} Tr[S_q^{bb'} \gamma_\nu \tilde{S}_Q^{aa'} \gamma_\mu] + 4S_Q^{ca'} \gamma_\nu \tilde{S}_q^{ab'} \gamma_\mu S_q^{bc'} + 4S_q^{ca'} \gamma_\nu \tilde{S}_Q^{ab'} \gamma_\mu S_Q^{bc'} \\ &\left. + 4S_q^{ca'} \gamma_\nu \tilde{S}_Q^{ab'} \gamma_\mu S_q^{bc'} \right\}, \end{aligned} \quad (11)$$

where $\tilde{S}_{q(Q)}^{ij} = C S_{q(Q)}^{ijT} C$. To go further in the calcula-

tions, the thermal light quark propagator in coordinate

space is selected as (see also [55, 56])

$$\begin{aligned}
S_q^{ij}(x) &= i \frac{\not{x}}{2\pi^2 x^4} \delta_{ij} - \frac{m_q}{4\pi^2 x^2} \delta_{ij} - \frac{\langle \bar{q}q \rangle_T}{12} \delta_{ij} \\
&- \frac{x^2}{192} m_0^2 \langle \bar{q}q \rangle_T \left[1 - i \frac{m_q}{6} \not{x} \right] \delta_{ij} \\
&+ \frac{i}{3} \left[\not{x} \left(\frac{m_q}{16} \langle \bar{q}q \rangle_T - \frac{1}{12} \langle u^\mu \Theta_{\mu\nu}^f u^\nu \rangle \right) \right. \\
&+ \left. \frac{1}{3} \left(u \cdot x \not{x} \langle u^\mu \Theta_{\mu\nu}^f u^\nu \rangle \right) \right] \delta_{ij} \\
&- \frac{i g_s \lambda_A^{ij}}{32\pi^2 x^2} G_{\mu\nu}^A \left(\not{x} \sigma^{\mu\nu} + \sigma^{\mu\nu} \not{x} \right) \\
&- i \frac{x^2 \not{x} g_s^2 \langle \bar{q}q \rangle_T^2}{7776} \delta_{ij} - \frac{x^4 \langle \bar{q}q \rangle_T \langle g_s^2 G^2 \rangle_T}{27648} + \dots, \tag{12}
\end{aligned}$$

which includes the thermal quark and gluon condensates ($\langle \bar{q}q \rangle_T$ and $\langle g_s^2 G^2 \rangle_T$), gluon fields in thermal bath, mixed condensate ($m_0^2 \langle \bar{q}q \rangle_T = \langle \bar{q}g_s \sigma Gq \rangle$) as well as new operators containing the energy momentum tensor, $\Theta_{\mu\nu}$. For the heavy quark, the following propagator including the thermal gluon condensate and gluon fields in hot medium is used [57]:

$$\begin{aligned}
S_Q^{ij}(x) &= i \int \frac{d^4 k e^{-ik \cdot x}}{(2\pi)^4} \left(\frac{\not{k} + m_Q}{k^2 - m_Q^2} \delta_{ij} \right. \\
&- \frac{g_s G_{ij}^{\alpha\beta}}{4} \frac{\sigma^{\alpha\beta} (\not{k} + m_Q) + (\not{k} + m_Q) \sigma^{\alpha\beta}}{(k^2 - m_Q^2)^2} \\
&+ \left. \frac{m_Q}{12} \frac{k^2 + m_Q \not{k}}{(k^2 - m_Q^2)^4} \langle g_s^2 G^2 \rangle_T \delta_{ij} + \dots \right). \tag{13}
\end{aligned}$$

In Eqs. (12) and (13), $m_q(Q)$ denotes the light(heavy) quark mass.

The thermal quark condensates, $\langle \bar{q}q \rangle_T$ (for $q = u, d$) and $\langle \bar{s}s \rangle_T$ are parameterized in terms of the vacuum condensates, $\langle 0 | \bar{q}q | 0 \rangle$ and $\langle 0 | \bar{s}s | 0 \rangle$. For these quantities, we use the following parametrizations in terms of temperature, which are based on the lattice QCD predictions [58]. Note that in this study the temperature dependence of these quantities are given up to a temperature $T = 300 \text{ MeV}$. However, we parameterize them up to $T_{pc} \approx 155 \text{ MeV}$, which is considered as the pseudo-critical temperature for the crossover phase transition at zero chemical potential. We get,

$$\frac{\langle \bar{q}q \rangle_T}{\langle 0 | \bar{q}q | 0 \rangle} = (A_1 e^{\frac{T}{0.025[GeV]}} + 1.015), \tag{14}$$

and

$$\frac{\langle \bar{s}s \rangle_T}{\langle 0 | \bar{s}s | 0 \rangle} = (A_2 e^{\frac{T}{0.019[GeV]}} + 1.002), \tag{15}$$

where $A_1 = -6.534 \times 10^{-4}$ and $A_2 = -2.169 \times 10^{-5}$. As we previously mentioned, because of the choice of the thermal rest frame in Wilson expansion, the Lorentz invariance is broken. To restore that the four-velocity vector of the medium $u^\mu = (1, 0, 0, 0)$ is introduced, which implies $u^2 = 1$ and $q \cdot u = q_0$. In the rest frame of heat bath, $\langle u^\mu \Theta_{\mu\nu}^{f,g} u^\nu \rangle = \langle u \Theta^{f,g} u \rangle = \langle \Theta_{00}^{f,g} \rangle = \langle \Theta^{f,g} \rangle$, as well. In thermal version, as also mentioned above, new operators representing the fermionic and gluonic parts of the energy-momentum tensor arises in OPE. The fermionic part $\Theta_{\mu\nu}^f$ appears explicitly in the light-quark propagator, while the gluonic part of the energy-momentum tensor $\Theta_{\lambda\sigma}^g$ appears in the expansion of the trace of two-gluon field strength tensor in heat bath [59]:

$$\begin{aligned}
\langle T r^c G_{\alpha\beta} G_{\mu\nu} \rangle &= \frac{1}{24} (g_{\alpha\mu} g_{\beta\nu} - g_{\alpha\nu} g_{\beta\mu}) \langle G^2 \rangle_T \\
&+ \frac{1}{6} \left[g_{\alpha\mu} g_{\beta\nu} - g_{\alpha\nu} g_{\beta\mu} - 2(u_\alpha u_\mu g_{\beta\nu} \right. \\
&- u_\alpha u_\nu g_{\beta\mu} - u_\beta u_\mu g_{\alpha\nu} + u_\beta u_\nu g_{\alpha\mu}) \left. \right] \\
&\times \langle u^\lambda \Theta_{\lambda\sigma}^g u^\sigma \rangle. \tag{16}
\end{aligned}$$

The temperature dependent gluon condensate $\langle G^2 \rangle_T$ is parameterized in terms of the vacuum gluon condensate $\langle 0 | G^2 | 0 \rangle$ [58] as:

$$\begin{aligned}
\delta \langle \frac{\alpha_s}{\pi} G^2 \rangle_T &= -\frac{8}{9} [\delta T_\mu^\mu(T) - m_u \delta \langle \bar{u}u \rangle_T \\
&- m_d \delta \langle \bar{d}d \rangle_T - m_s \delta \langle \bar{s}s \rangle_T], \tag{17}
\end{aligned}$$

where the vacuum subtracted values of the consider quantities are used as $\delta f(T) \equiv f(T) - f(0)$ and $\delta T_\mu^\mu(T) = \varepsilon(T) - 3p(T)$: $\varepsilon(T)$ is the energy density and $p(T)$ is the pressure. Taking into account the recent Lattice calculations [60, 61] we get the fit function of $\delta T_\mu^\mu(T)$ as

$$\frac{\delta T_\mu^\mu(T)}{T^4} = (0.020 \times e^{\frac{T}{0.034[GeV]}} + 0.115). \tag{18}$$

For the temperature-dependent strong coupling [62, 63] we utilize

$$g_s^{-2}(T) = \frac{11}{8\pi^2} \ln \left(\frac{2\pi T}{\Lambda_{\overline{MS}}} \right) + \frac{51}{88\pi^2} \ln \left[2 \ln \left(\frac{2\pi T}{\Lambda_{\overline{MS}}} \right) \right], \tag{19}$$

where, $\Lambda_{\overline{MS}} \simeq T_{pc}/1.14$.

Alike to the physical part, the correlation function on the OPE side is expanded in terms of the Lorentz structures as

$$\begin{aligned}
\Pi_{\mu\nu}^{OPE}(q, T) &= \Gamma_1^{OPE} \not{q} g_{\mu\nu} + \Gamma_2^{OPE} g_{\mu\nu} \\
&+ \text{other structures}, \tag{20}
\end{aligned}$$

where $\Gamma_{1(2)}^{OPE}$ is the coefficient of the selected Lorentz structure. These functions can be expressed by the help of following dispersion integral:

$$\Gamma_{1(2)}^{OPE} = \int_{s_{min}}^{\infty} ds \frac{\rho_{1(2)}^{OPE}(s, T)}{s - q^2} + \Gamma_{1(2)}^{nonpert}, \quad (21)$$

where $s_{min} = (m_{q_1} + m_{q_2} + m_Q)^2$, $\rho_{1(2)}^{OPE}(s, T)$ is the spectral density obtained via the imaginary part of the perturbative correlation function (*pert* in the following equation stands for the perturbative contributions)

$$\rho_{1(2)}^{OPE}(s, T) = \frac{1}{\pi} \text{Im}[\Gamma_{1(2)}^{OPE, pert}], \quad (22)$$

and $\Gamma_{1(2)}^{nonpert}$ represents the contributions coming from all the nonperturbative effects. In this step, our main aim is to calculate the spectral densities, corresponding to the perturbative effects in the present study, as well as the nonperturbative contributions to the QCD side. To this end, the explicit forms of the heavy and light quark propagators are inserted into Eqs. (10) and (11). The next step is to perform the standard but lengthy calculations: These calculations contain Fourier integrals appearing in different forms, Borel transformation as well as continuum subtraction. By matching the coefficients of the se-

lected structures from both the physical and OPE sides of the correlation function, we find the desired sum rules:

$$\lambda_{B_{SH}}^2(T) e^{-m_{B_{SH}}^2(T)/M^2} = \hat{B}\Gamma_1^{OPE}, \quad (23)$$

and

$$\lambda_{B_{SH}}^2(T) m_{B_{SH}}(T) e^{-m_{B_{SH}}^2(T)/M^2} = \hat{B}\Gamma_2^{OPE}, \quad (24)$$

where the functions $\hat{B}\Gamma_{1(2)}^{OPE}$ denote the $\Gamma_{1(2)}^{OPE}$ in Borel scheme and are given as

$$\hat{B}\Gamma_{1(2)}^{OPE} = \int_{s_{min}}^{s_0(T)} ds \rho_{1(2)}^{OPE}(s, T) e^{-s/M^2} + \hat{B}\Gamma_{1(2)}^{nonpert}, \quad (25)$$

with $s_0(T)$ being the temperature-dependent continuum threshold. We will use the above sum rules to extract the values of the mass and residue of the baryons under consideration as well as their thermal behavior in next section.

As examples, we would like to present the explicit forms of the $\rho_1^{OPE}(s, T)$ and $\hat{B}\Gamma_1^{nonpert}$ for the Σ_b^* baryon. They are obtained as

$$\begin{aligned} \rho_1^{OPE}(s, T) = & \frac{-1}{96\pi^4\beta} \int_0^1 dz \left\{ z(m_b^2 + s\beta) \left[z(3m_b^2(z+1) - 12m_b m_u + s\beta(7z+3)) \right. \right. \\ & \left. \left. - 12m_d(m_b z - 2m_u\beta) \right] \right\} \Theta[L(s, z)], \end{aligned} \quad (26)$$

and

$$\begin{aligned}
\hat{B}\Gamma_1^{\text{nonpert}} &= \frac{-1}{1152\pi^4} \int_{s_{\min}}^{s_0(T)} ds \int_0^1 dz \left\{ -96\pi^2 \left\{ \langle \bar{d}d \rangle \left[2z(-2m_b + m_d + 2m_u) - 3m_d z^2 + m_d - 4m_u \right] \right. \right. \\
&+ \langle \bar{u}u \rangle \left[-4m_b z + 4\beta m_d + m_u(2 - 3z)z + m_u \right] \left. \right\} + g_s^2 \left(\langle G^2 \rangle \left[(43 - 6z)z + 2 \right] \right. \\
&+ \left. 2 \langle u\Theta^g u \rangle [z(21z + 23) + 15] + 256\pi^2 \beta \langle u\Theta^f u \rangle (5z - 1) \right) \Theta[L(s, z)] \\
&+ \int_0^1 dz e^{\frac{m_b^2}{M^2\beta}} g_s^2 \left\{ \frac{-1}{1152\pi^4 M^2 \beta^2} \left(m_b^2 z \langle G^2 \rangle \left\{ z(2m_b(m_d + m_u) + M^2) - 4m_d m_u \right\} \right) \right. \\
&+ \frac{1}{13824\pi^2 M^6 \beta^3} \left(\langle \bar{d}d \rangle \left\{ \langle G^2 \rangle \left[-16m_b^4 m_d z + 8m_b^3 \beta(m_d m_u + 2M^2 z) - 4m_b^2 M^2 \beta(5m_d(3z + 1) - 4m_u) \right. \right. \right. \\
&+ \left. \left. 8m_b M^2 \beta(2m_d m_u(3z - 2) + M^2(z(10z - 3) - 3)) + 119m_d M^4 \beta^3 \right] + 8M^2 \beta^2 \langle u\Theta^g u \rangle (6m_b^2 m_d - 12m_b M^2 \right. \\
&+ \left. m_d \beta(31M^2 - 8q_0^2) \right) \left. \right\} + \langle \bar{u}u \rangle \left\{ \langle G^2 \rangle \left[-16m_b^4 m_u z + 8m_b^3 \beta(m_d m_u + 2M^2 z) + 4m_b^2 M^2 \beta(4m_d - 5(3m_u z + m_u)) \right. \right. \\
&+ \left. \left. 8m_b M^2 \beta(2m_d m_u(3z - 2) + M^2(z(10z - 3) - 3)) + 119m_u M^4 \beta^3 \right] + 8M^2 \beta^2 \langle u\Theta^g u \rangle (6m_b^2 m_u - 12m_b M^2 \right. \\
&+ \left. m_u \beta(31M^2 - 8q_0^2) \right) \left. \right\} + \frac{1}{663552\pi^4 M^6 \beta^3} \left(m_b^2 \langle G^2 \rangle^2 g_s^2 \left\{ 32m_b^2 z + M^2 \beta(187z + 16) \right\} \right. \\
&+ 4 \langle G^2 \rangle \left\{ 64\pi^2 \langle u\Theta^f u \rangle \left[8m_b^4 z - 2m_b^3 \beta(m_d + m_u) - 2m_b^2 \beta(M^2(z - 5) - 32q_0^2 z) \right. \right. \\
&- \left. \left. 4m_b M^2 \beta(3z - 2)(m_d + m_u) - 55M^4 \beta^3 \right] - m_b^2 g_s^2 \langle u\Theta^g u \rangle (16m_b^2 z \right. \\
&+ \left. M^2 \beta(85z - 16)) \right\} - 3072\pi^2 M^2 \beta^2 \langle u\Theta^f u \rangle \langle u\Theta^g u \rangle (2m_b^2 + \beta(5M^2 + 8q_0^2)) \left. \right) \left. \right\} \Theta[L(s_0, z)] \\
&+ \frac{e^{-\frac{m_b^2}{M^2}}}{\pi^2} \left\{ \frac{m_0^2}{72M^2} \left(\langle \bar{d}d \rangle [2m_b m_d m_u + M^2(m_d - 6m_u)] + \langle \bar{u}u \rangle [2m_b m_d m_u + M^2(m_u - 6m_d)] \right) \right. \\
&- \frac{1}{972M^4} \left(\langle \bar{u}u \rangle \left[27\pi^2 \langle \bar{d}d \rangle (3m_b^2 m_d m_u - 8m_b M^2(m_d + m_u) + 2M^2(3m_d m_u + 8M^2)) \right. \right. \\
&+ \left. \left. 4M^2 g_s^2 \langle \bar{u}u \rangle (m_b(m_d + m_u) + M^2) \right) \right) + \frac{1}{6912M^2} \left(\langle \bar{d}d \rangle \left[13m_d M^2 \langle G^2 \rangle g_s^2 + 52m_d M^2 g_s^2 \langle u\Theta^g u \rangle \right. \right. \\
&+ \left. \left. 512\pi^2 \langle u\Theta^f u \rangle (3m_b^2 m_d - 4m_b M^2 - 4m_d(M^2 + 2q_0^2)) \right) \right) + \langle \bar{u}u \rangle \left[\langle G^2 \rangle g_s^2 (16m_b^2(m_d + m_u) \right. \\
&+ \left. M^2(32m_b + 16m_d + 35m_u)) + 76m_u M^2 g_s^2 \langle u\Theta^g u \rangle + 512\pi^2 \langle u\Theta^f u \rangle (3m_b^2 m_u - 4m_b M^2 - 12m_u(M^2 + 2q_0^2)) \right] \\
&+ \frac{1}{162M^8} \left(3\pi^2 m_0^2 \langle \bar{d}d \rangle \langle \bar{u}u \rangle \left[3m_b^4 m_d m_u - 5m_b^3 M^2(m_d + m_u) + 3m_b^2 M^2(4M^2 - m_d m_u) + 3M^4(4M^2 - m_d m_u) \right] \right. \\
&\left. \left. - M^4 \langle u\Theta^f u \rangle \left[M^2 \langle G^2 \rangle g_s^2 + 4M^2 g_s^2 \langle u\Theta^g u \rangle + 16\pi^2 \langle u\Theta^f u \rangle (3m_b^2 + 8M^2 + 16q_0^2) \right] \right) \right\}, \tag{27}
\end{aligned}$$

where Θ stands for the unit-step function, $L(s, z) = s z(1 - z) - m_b^2 z$ and $\beta = z - 1$.

III. NUMERICAL RESULTS

In this section, we analyze the obtained sum rules for the masses and residues. They includes some input pa-

parameters such as the heavy and light quark masses, m_0^2 , quark and gluon condensates in vacuum and energy of the quasi-particle in medium, q_0 . Their numerical values are presented in Table II.

Parameter	Numeric Value
$q_0^{\Sigma_b^*}; q_0^{\Sigma_c^*}$	$(5832.1 \pm 1.9) MeV; (2518.48 \pm 0.20) MeV$
$q_0^{\Xi_b^*}; q_0^{\Xi_c^*}$	$(5949 \pm 1.9) MeV; (2646.32 \pm 0.31) MeV$
$q_0^{\Omega_b^*}; q_0^{\Omega_c^*}$	$(6.08 \pm 0.40) GeV; (2765.9 \pm 2.0) MeV$
$m_u; m_d$	$(2.2_{-0.4}^{+0.5}) MeV; (4.7_{-0.3}^{+0.7}) MeV$
m_s	$(95_{-3}^{+9}) MeV$
$m_b; m_c$	$(4.18_{-0.03}^{+0.04}) GeV; (1.275_{-0.035}^{+0.025}) GeV$
$m_0^2;$	$(0.8 \pm 0.2) GeV^2$
$\langle 0 \bar{q}q 0 \rangle (q = u, d)$	$-(272(5) MeV)^3$
$\langle 0 \bar{s}s 0 \rangle$	$-(296(11) MeV)^3$
$\langle 0 \frac{1}{\pi} \alpha_s G^2 0 \rangle$	$0.028(3) GeV^4$

TABLE II: Input parameters used in calculations [58, 64–67].

In addition, we also need to have the gluonic and fermionic parts of the energy density. Based on the lattice QCD results on the thermal behavior of the energy-momentum tensor given in [60], their parametrizations, up to the pseudo-critical point under consideration in the present study, are obtained as

$$\frac{\langle \Theta^f \rangle}{T^4} = (0.009 \times e^{\frac{T}{0.0402[GeV]}} + 0.024), \quad (28)$$

$$\frac{\langle \Theta^g \rangle}{T^4} = (0.091 \times e^{\frac{T}{0.047[GeV]}} - 0.731), \quad (29)$$

which, we are going to use them in our numerical computations. The next problem is to obtain the parametrization of $s_0(T)$ as a function of temperature. This function shall reduce to the vacuum threshold, s_0 , at zero temperature. We parameterize it as

$$s_0(T) = s_0 f(T), \quad (30)$$

such that at $T \rightarrow 0$ limit, $f(T) \rightarrow 1$. Hence, we should first determine s_0 based on the standard prescriptions of the method, afterwards we will extract the function $f(T)$ from the calculations.

Besides the continuum threshold in vacuum the sum rules obtained in previous section include another auxiliary parameter, Borel parameter M^2 , which should also be fixed. We need to determine the working regions of s_0 and M^2 such that the physical quantities under consideration show mild dependence on these parameters. The continuum threshold s_0 is not totally free but it is related to the energy of the first excited state in the same channel. Thanks to the experiments that have provided many new results not only on the ground states but also on the excited states of some single heavy baryons, recently [67]. In view of PDG, we see that the excited states generally have energies about 300 MeV above the ground states masses. In choosing the working window for the s_0 , we also look after the pole dominance and OPE convergence in our sum rules. These considerations leads to the window:

$$[m_{B_{SH}} + 0.3]^2 GeV^2 \leq s_0 \leq [m_{B_{SH}} + 0.5]^2 GeV^2. \quad (31)$$

The upper and lower limits of the Borel parameter are fixed consider the criteria of the QCD sum rule method. To find the lower limit, we apply the criterion of the OPE convergence at the chosen window for the continuum threshold. To this end, we demand that the perturbative part exceeds the total nonperturbative contributions and the slogan of *the higher the dimension of the nonperturbative operator the lower its contribution* is satisfied. Our calculations show that the operators having eight dimensions, the higher dimension that we include into the analyses, constitute only one percent of the total contribution at lower value of M^2 , i.e. $\Gamma_{1(2)}^{8,OPE}(M_{min}^2, s_0)/\Gamma_{1(2)}^{total,OPE}(M_{min}^2, s_0) \simeq 0.01$. Figure 2 shows the perturbative and nonperturbative contributions to total OPE as well as the contributions of different nonperturbative operators with various mass dimensions, separately. This figure depicts a nice convergence of the OPE in our calculations. As it is clear, the perturbative contribution dominates over nonperturbative contributions and it is about 53% of the total at $M_{min}^2 = 6 GeV^2$. The main contribution in nonperturbative part belongs to the quark condensate, $\langle \bar{q}q \rangle$.

To obtain M_{max}^2 , we utilize the condition of the pole

dominance as

$$PC = \frac{\Gamma_{1(2)}^{OPE}(M^2, s_0)}{\Gamma_{1(2)}^{OPE}(M^2, \infty)} \geq \frac{1}{2}. \quad (32)$$

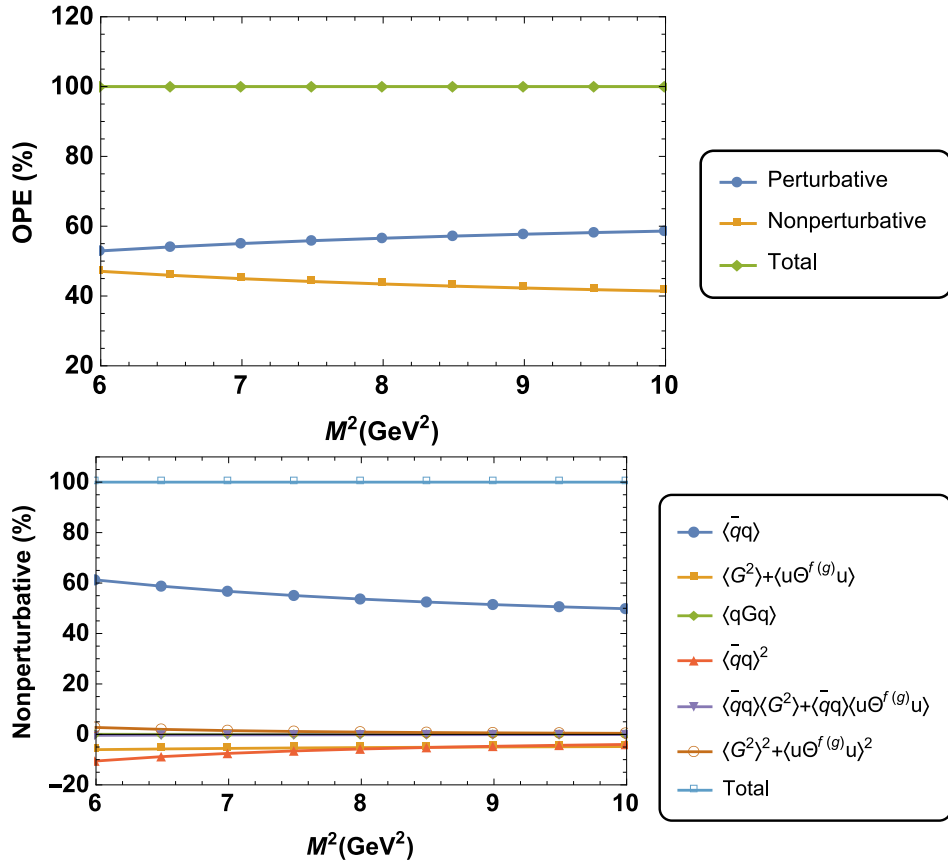


FIG. 2: Up: Contributions of perturbative and nonperturbative parts to total OPE. Down: Contributions of various operators with different dimensions to nonperturbative part: $\langle \bar{q}q \rangle$ (dimension 3), $\langle G^2 \rangle + \langle u\Theta^{f(g)}u \rangle$ (dimension 4), $\langle qGq \rangle$ (dimension 5), $\langle \bar{q}q \rangle^2$ (dimension 6), $\langle \bar{q}q \rangle \langle G^2 \rangle + \langle \bar{q}q \rangle \langle u\Theta^{f(g)}u \rangle$ (dimension 7), $\langle G^2 \rangle^2 + \langle u\Theta^{f(g)}u \rangle^2$ (dimension 8).

As a result, we get the working region of the Borel parameter as $M^2 \in [6, 10] \text{ GeV}^2$. We plot, as an example, a 3D graphic of the mass of Σ_b^* baryon as functions of M^2 and s_0 at $T = 0$ in Figure 3. As is seen the mass shows good stability against the variations of the auxiliary parameters in the selected windows.

Now, we proceed to find the function $f(T)$ and the temperature dependent mass $m_{B_{SH}}(T)$ and residue $\lambda_{B_{SH}}(T)$ of the single heavy spin-3/2 baryons. To this end, we use the two sum rules in Eqs. (23) and (24) and one extra equation obtained by applying the derivative with respect to $\frac{d}{d(-\frac{1}{M^2})}$ to both sides of Eq. (23). Simultaneous solving of the resultant three equations with the aim of obtaining the three mentioned unknowns gives the function $f(T)$ as

$$f(T) = 1 - 0.96 \left(\frac{T}{T_{pc}} \right)^9. \quad (33)$$

In the following, we proceed to discuss the thermal behavior of the masses and residues under study as the main

goal of the present work. In this context, as examples, we plot the $m(T)/m(0)$ and $\lambda(T)/\lambda(0)$ for the bottom members as functions of T/T_{pc} and M^2 in Figure 4 at average value of the vacuum continuum threshold. This figure shows that the spectroscopic parameters of the Σ_b^* , Ξ_b^* and Ω_b^* baryons are stable against the changes in temperature until a certain temperature but after that, they start to decrease with increasing the temperature. Our analyses show that the charmed baryons present similar behavior, as well. The points that the stability starts to break down for mass and residue are $T \cong 0.14 \text{ GeV}$ and $T \cong 0.13 \text{ GeV}$, respectively. After these points the mass and residue starts to diminish. The mass and residue fall substantially near to the pseudo-critical temperature. The amount of decrements at T_{pc} are 75% (66–71%) for the mass of bottom (charmed) and 71–80% (42–50%) for the residue of bottom (charmed) baryons, respectively compared to their vacuum values. These behavior of baryons can be interpreted as substantial melting of the

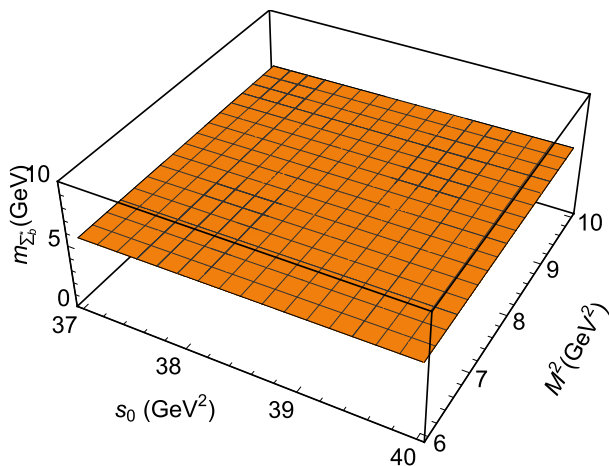


FIG. 3: The mass of the Σ_b^* baryon as functions of M^2 and s_0 at $T = 0$.

At the end of this section, we would like to present our results for the masses of the single heavy spin-3/2 baryons at $T \rightarrow 0$ limit. This is done in table III. For comparison, we also present the existing theoretical predictions in the literature and experimental data in the same table. With a quick glance in this table, we see that our predictions, within the errors, are overall consistent with other theoretical predictions made using different

heavy baryons near to the pseudo-critical temperature.

methods and approaches. Our predictions are also well consistent with the existing experimental data for five members within the presented uncertainties. Ω_b^* baryon is only missing member, which has not been discovered in the experiment. We hope that, our result together with other theoretical predictions will help experimental group in the course of search for this particle.

IV. SUMMARY AND CONCLUDING REMARKS

In this study, we have performed two-point thermal QCD sum rule analyses for Σ_Q^* , Ξ_Q^* and Ω_Q^* single heavy baryons which are the members of the spin-3/2 sextet family. In the OPE, operators up to dimension eight were taken into account which lead to a good OPE convergence as well as pole dominance. We included the thermal effects by two ways: We replaced the vacuum condensates by their thermal versions and considered the extra operators, appearing in the forms of the fermionic and gluonic parts of the energy momentum tensor due to the restoration of the Lorentz invariance. We fixed the auxiliary parameters entering the calculations by the standard prescriptions of the method. By simultaneous solving of the two sum rules obtained together with an extra equation derived from one of the sum rules, we found three

unknowns: Thermal continuum threshold, temperature-dependent mass and temperature-dependent residue. We discussed the thermal behavior of the mass and residue for all the bottom and charmed baryon members having the spin-3/2. We observed that the spectroscopic parameters remain unchanged up to a certain temperature, after which they start to diminish considerably near to the pseudo-critical temperature. The decrements order in the mass and residue of the considered baryons near to the pseudo-critical temperature are obtained as (66–75)% and (42–80)%, respectively, representing substantial melting of the heavy baryons near to the pseudo-critical temperature. In the literature, there are no other studies on the thermal behavior of single heavy baryons to make a comparison with our predictions. However, there are some studies on the temperature dependence of the masses of light baryons, In Refs. [55, 68] the authors investigated the light octet and decuplet baryons using

	$m_{\Omega_b^*}$	$m_{\Omega_c^*}$	$m_{\Sigma_b^*}$	$m_{\Sigma_c^*}$	$m_{\Xi_b^*}$	$m_{\Xi_c^*}$
present work	$6.08^{+0.10}_{-0.15}$	$2.75^{+0.08}_{-0.26}$	$5.88^{+0.11}_{-0.11}$	$2.56^{+0.08}_{-0.07}$	$5.95^{+0.12}_{-0.13}$	$2.65^{+0.08}_{-0.07}$
[15]	-	-	5.805	2.495	-	-
[16]	-	-	$5.4 \sim 6.2$	$2.15 \sim 2.92$	-	-
[18]	-	2.768	-	2.518	-	-
[19]	6.090 ± 0.050	2.770 ± 0.030	5.850 ± 0.040	2.520 ± 0.020	5.980 ± 0.040	2.650 ± 0.020
[20]	6.083	2.760	5.840	-	5.966	-
[21]	-	-	5.84 ± 0.09	2.55 ± 0.08	-	-
[23]	-	-	5.82 ± 0.13	2.59 ± 0.20	-	-
[24]	6.060	2.752	5.871	2.538	5.959	2.680
[26]	6.088	2.768	5.834	2.518	5.963	2.654
[28, 34]	6.00 ± 0.16	2.74 ± 0.23	5.81 ± 0.19	2.56 ± 0.24	5.94 ± 0.17	2.64 ± 0.22
[29]	6.06 ± 0.13	2.76 ± 0.10	-	-	-	-
[31]	6.079	2.767	5.829	2.502	5.961	2.642
[32]	$6.063^{+0.083}_{-0.082}$	$2.790^{+0.109}_{-0.105}$	$5.835^{+0.082}_{-0.077}$	$2.534^{+0.096}_{-0.081}$	$5.929^{+0.083}_{-0.079}$	$2.634^{+0.102}_{-0.094}$
[35]	-	-	5.829	-	-	-
[36]	6.082	-	-	-	5.959 ± 0.004	-
[37]	6.08 ± 0.40	2.72 ± 0.20	5.85 ± 0.35	2.51 ± 0.15	5.97 ± 0.40	2.66 ± 0.18
[38]	6.044 ± 0.018	-	5.842 ± 0.026	-	5.950 ± 0.021	-
[39]	6.17 ± 0.15	2.79 ± 0.19	5.85 ± 0.20	2.48 ± 0.25	6.02 ± 0.17	2.65 ± 0.20
[40]	6.088	2.768	5.834	2.519	5.963	2.649
[41]	6.073	-	5.834	-	5.954	-
Exp[3]	-	2.7659 ± 0.0020	5.83032 ± 0.00027	2.51848 ± 0.00020	5.9523 ± 0.0009	2.64638 ± 0.00021

TABLE III: The vacuum mass comparison of the single heavy spin-3/2 baryons in GeV with existing theoretical predictions and experimental data (Exp[3]).

the thermal QCD sum rule, but considering a pseudo-critical temperature of $T_{pc} = 197 MeV$. They obtained that the shifts in the masses of the considered baryons are overall about 80%. The pole mass of the octet and decuplet baryons were also evaluated in Ref. [69] via the chiral perturbation theory. The authors observed that a 20% mass shift occurs around the temperature $T \simeq 150 MeV$, where the freeze-out in the relativistic heavy-ion collision is expected to be formed. Using the many-body techniques at finite temperature, all baryonic states of the octet and decuplet flavors were examined in Ref. [70]. They obtained that the baryon masses decrease with the temperature and there are strong dependencies on the melting (or deconfinement) temperature depending on the flavor content of the baryons. In the framework of the thermal QCD sum rule, the masses of the decuplet baryons were also investigated in Ref. [71]. According to this study, the masses of the decuplet baryons show very little temperature dependence below $T = 0.11 GeV$ and the melting or hadron-quark phase transition occurs at

a temperature $T \geq 0.11 GeV$. Our results indicate that this point is $T = 0.14 GeV$ for heavy baryons, after which the masses start to decrease with the increasing of the temperature and the dependence of the masses on temperature near to the critical temperature is very strong. These information on the behavior of the masses of different baryons may help experimental groups in the analyses of the results of the in-medium and heavy ion collision experiments, despite the statistical hadronization model claims that any thermal modification of masses is negligibly small at pseudo-critical temperature and the in-medium mass shifts at T_{pc} would be excluded.

We extracted the values of the masses for both the bottom and charmed baryons at $T \rightarrow 0$ limit and compared with the predictions of other phenomenological models and experimental data. The obtained results are well consistent with existing experimental data. Our result on the mass of Ω_b^* baryon as the only undiscovered member together with other predictions may help the experimental group to hunt this particle and measure its pa-

rameters.

-
- [1] N. Isgur and M. B. Wise, Phys. Lett. B **232**, 113, (1989),
N. Isgur and M. B. Wise, Phys. Rev. Lett. **66**, 1130, (1991).
- [2] H. Georgi, Phys. Lett. B **240**, 447 (1990).
- [3] M. Tanabashi et al. (Particle Data Group), Phys. Rev. D **98**, 030001 (2018).
- [4] D. Acosta et al., (CDF Collaboration), Phys. Rev. Lett. **96**, 202201 (2006).
- [5] B. Aubert et al., (BABAR Collaboration), Phys. Rev. Lett. **97**, 232001 (2006).
- [6] T. Aaltonen et al., (CDF Collaboration), Phys. Rev. Lett. **99**, 202001 (2007).
- [7] V. Abazov et al., (D0 Collaboration), Phys. Rev. Lett. **99**, 052001 (2007).
- [8] T. Aaltonen et al., (CDF Collaboration), Phys. Rev. Lett. **99**, 052002 (2007).
- [9] R. Chistov et al., (Belle Collaboration), Phys. Rev. Lett. **97**, 162001 (2006).
- [10] B. Aubert et al., (BABAR Collaboration), Phys. Rev. D **77**, 012002 (2008).
- [11] T. Lesiak et al., (Belle Collaboration), Phys. Lett. B **665**, 9 (2008).
- [12] S. Chatrchyan et al., (CMS Collaboration), Phys.Rev.Lett. **108**, 252002 (2012).
- [13] R. Aaij et al., (LHCb Collaboration), JHEP **1605**, 161 (2016).
- [14] E. V. Shuryak, Nucl. Phys. B **198**, 83 (1982).
- [15] S. Capstick and N. Isgur, Phys. Rev. D **34**, 2809 (1986).
- [16] E. Bagan, M. Chabab, H. G. Dosch, and S. Narison, Phys. Lett. B **278**, 367 (1992).
- [17] A. G. Grozin and O. I. Yakovlev, Phys. Lett. B **285**, 254 (1992).
- [18] M. J. Savage, Phys. Lett. B **359**, 189 (1995).
- [19] R. Roncaglia, D. B. Lichtenberg, and E. Predazzi, Phys. Rev. D **52**, 1722 (1995); R. Roncaglia, A. Dzierba, D. B. Lichtenberg, and E. Predazzi, Phys. Rev. D **51**, 1248 (1995).
- [20] E. Jenkins, Phys. Rev. D **54**, 4515 (1996).
- [21] Y. B. Dai, C. S. Huang, C. Liu and C. D. Lu, Phys. Lett. B **371**, 99 (1996).
- [22] S. Groote, J. G. Körner and O. I. Yakovlev, Phys. Rev. D **55**, 3016 (1997).
- [23] D. W. Wang, M. Q. Huang and C. Z. Li, Phys. Rev. D **65**, 094036 (2002).
- [24] N. Mathur, R. Lewis, and R. M. Woloshyn, Phys. Rev. D **66**, 014502 (2002).
- [25] D. W. Wang, M. Q. Huang, Phys.Rev. D **67**, 074025 (2003).
- [26] D. Ebert, R. N. Faustov, and V. O. Galkin, Phys. Rev. D **72**, 034026 (2005).
- [27] H. Garcilazo, J. Vijande and A. Valcarce, J. Phys. G **34**, 961 (2007).
- [28] J. R. Zhang and M. Q. Huang, Phys. Rev. D **78**, 094015 (2008).
- [29] Z. G. Wang, Eur. Phys. J. C **54**, 231 (2008).
- [30] W. Roberts and M. Pervin, Int. J. Mod. Phys. A **23**, 2817 (2008).
- [31] A. Valcarce, H. Garcilazo and J. Vijande, Eur. Phys. J. A **37**, 217 (2008).
- [32] X. Liu, H. X. Chen, Y. R. Liu, A. Hosaka, and S. L. Zhu, Phys. Rev. D **77**, 014031 (2008).
- [33] S. Groote, J.G. Korner, A.A. Pivovarov, Eur.Phys.J.C **58**, 355 (2008).
- [34] J. R. Zhang and M. Q. Huang, Phys. Rev. D **77**, 094002 (2008).
- [35] S. M. Gerasyuta, E. E. Matskevich, Int.J. Mod.Phys. E **18**, 1785 (2009).
- [36] M. Karliner, B. Keren-Zura, H. J. Lipkin, and J. L.Rosner, Annals Phys. **324**, 2 (2009).
- [37] T. M. Aliev, K. Azizi, and A. Ozpineci, Nucl. Phys. B **808**,137 (2009).
- [38] R. Lewis, R.M. Woloshyn, Phys. Rev. D **79**, 014502 (2009).
- [39] Z. G. Wang, Eur. Phys. J. C **68**, 459 (2010).
- [40] D. Ebert, R. N. Faustov and V. O. Galkin, Phys. Rev. D **84**, 014025 (2011).
- [41] J.Y. Kim, H. C. Kim, G.S. Yang, Phys. Rev. D **98**, 054004 (2018).
- [42] K. Azizi, N. Er, Nucl.Phys. A **970**, 422 (2018).
- [43] Y. Aoki, G. Endrodi, Z. Fodor, S.D. Katz, K.K. Szabo, Nature **443**, 675-678, (2006).
- [44] M. Cheng et al., Phys. Rev. D **74**, 054507 (2006).
- [45] T. Bhattacharya et al., Phys. Rev. Let. (PRL) **113**, 082001 (2014).
- [46] A. Bazavov et al., Phys. Rev. D **95**, 054504 (2017).
- [47] M. A. Shifman, A. I. Vainstein, V. I. Zakharov, Nucl. Phys. B **147**, 385 (1979); M. A. Shifman, A. I. Vainstein, V. I. Zakharov, Nucl. Phys. B **147**, 448 (1979).
- [48] B. L. Ioffe, Nucl. Phys. B **188**, 317 (1981).
- [49] A. I. Bochkarev, M. E. Shaposhnikov, Nucl. Phys. B **268**, 220 (1986).
- [50] T. M. Aliev, M. Savci, Phys.Rev. D **90**, 116006, 11 (2014).
- [51] K. G. Savvidy, (2005) [arXiv:1005.3455 [hep-th]].
- [52] T. M. Aliev, K. Azizi and M. Savci, Phys. Rev. D **82**, 096006 (2010).
- [53] T. M. Aliev, K. Azizi and M. Savci, Phys. Lett. B **681**, 240 (2009) .

- [54] F. X. Lee, Phys. Rev. D **57**, 1801 (1998).
- [55] K. Azizi, G. Kaya, J. Phys. G **43**, no.5, 055002 (2016).
- [56] K. Azizi, A. Türkan, E. Veli Veliev, H. Sundu, Adv. High Energy Phys. **2015**, 794243 (2015).
- [57] L. J. Reinders, H. Rubinstein and S. Yazaki, Phys. Rept. **127**, 1 (1985).
- [58] P. Gubler, D. Satow, Prog. Part. Nucl. Phys. **106**, 1 (2019) [arXiv:1812.00385 [hep-ph]].
- [59] S. Mallik, Phys. Lett. B **416**, 373 (1998).
- [60] A. Bazavov et al., Phys. Rev., D **90**, 094503 (2014).
- [61] S. Borsanyi et al., Phys. Lett. B **730**, 99104 (2014).
- [62] O. Kaczmarek, F. Karsch, F. Zantow, P. Petreczky, Phys. Rev. D **70**, 074505 (2004).
- [63] K. Morita, S. H. Lee, Phys. Rev. C **77**, 064904 (2008).
- [64] V. M. Belyaev, B. L. Ioffe, Sov. Phys. JETP, **57**, 716 (1983).
- [65] H. G. Dosch, M. Jamin and S. Narison, Phys. Lett. B **220**, 251 (1989).
- [66] B. L. Ioffe, Prog. Part. Nucl. Phys. **56**, 232 (2006).
- [67] M. Tanabashi et al., Phys. Rev. D **98**, 030001 (2018).
- [68] K. Azizi, G. Bozkir, Eur. Phys. J. C **76**, 521 (2016).
- [69] P. F. Bedaque, Phys. Lett. B **387**, 1 (1996).
- [70] J. M. Torres-Rincon, B. Sintès, J. Aichelin, Phys. Rev. C **91**, 065206 (2015).
- [71] Y. Xu, Y. Liu, M. Huang, Commun. Theor. Phys. **63**, 209 (2015).

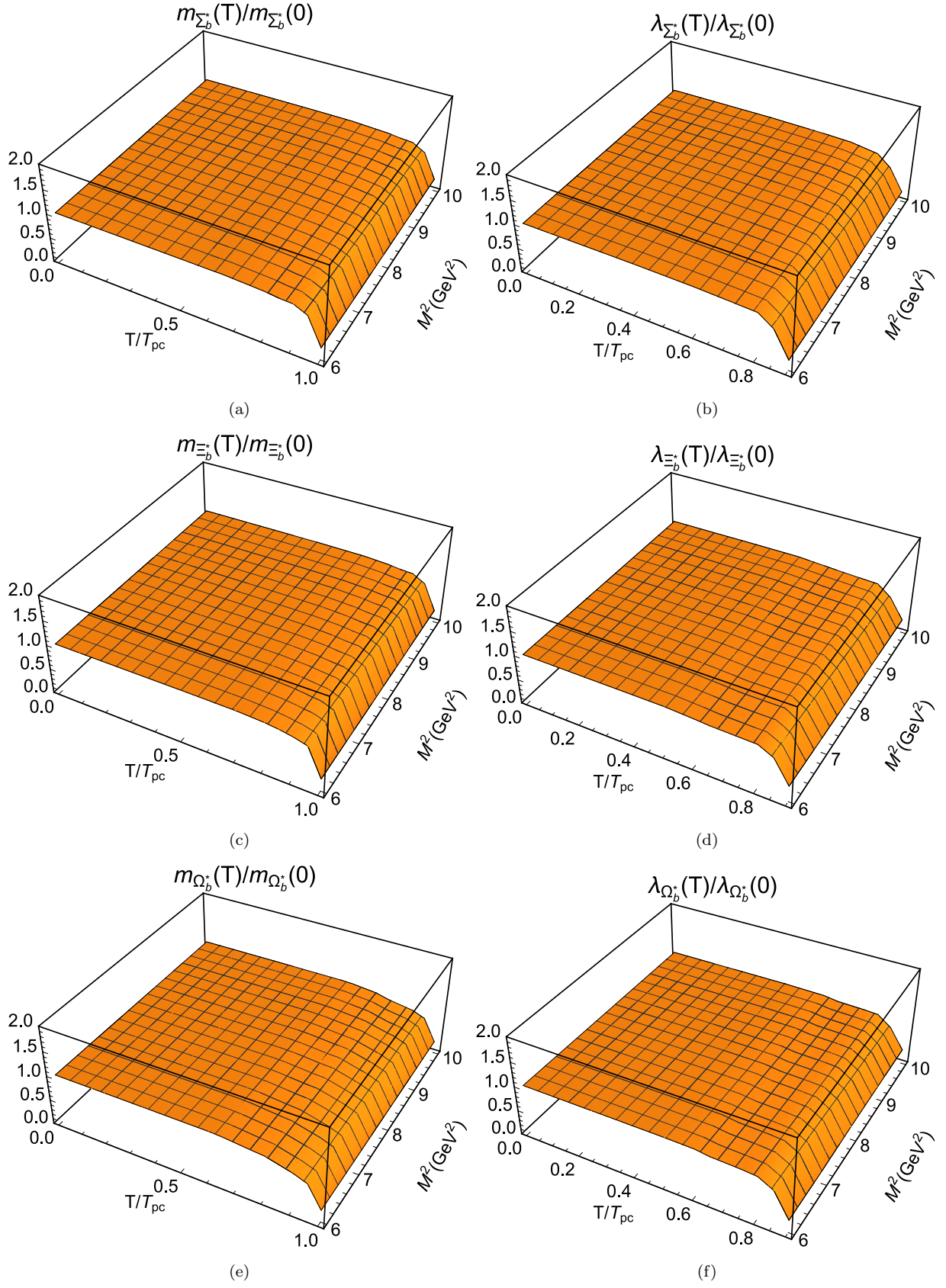


FIG. 4: The mass (right) and residue (left) of the bottom baryons as functions of M^2 and T/T_{pc} .